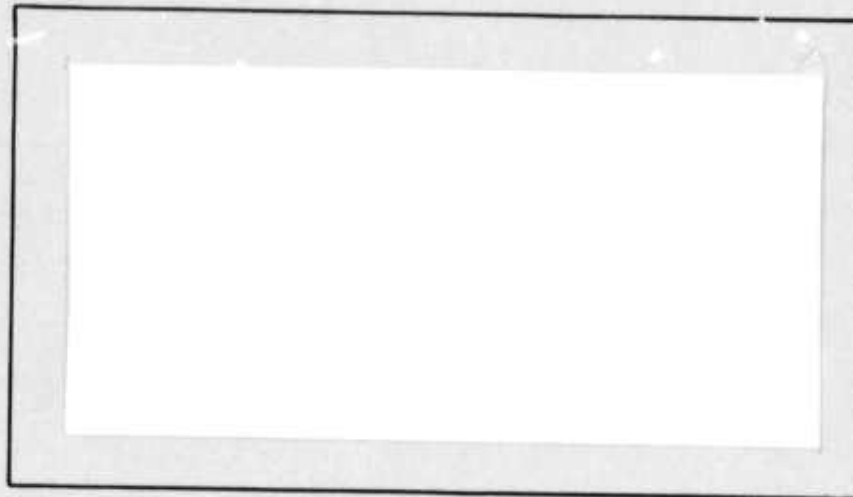


AD A 044953

AIR FORCE INSTITUTE OF TECHNOLOGY



AIR UNIVERSITY
UNITED STATES AIR FORCE



AD No. _____
DDC FILE COPY.

SCHOOL OF ENGINEERING

WRIGHT-PATTERSON AIR FORCE BASE, OHIO

AFLC-WPAF3-SEP 65 6M

DISTRIBUTION STATEMENT A

Approved for public release;
Distribution Unlimited

DDC
RECEIVED
OCT 5 1977
RECEIVED



QUANTITATIVE ANALYSIS OF RADIOACTIVE
NOBLE GASES WITH A SiLi DETECTOR
THESIS

GNE/PH/74-8 ✓

Charles E. Rowe
2Lt. USAF

Approved for public release and sale. Distribution unlimited.

6
QUANTITATIVE ANALYSIS OF RADIOACTIVE
NOBLE GASES WITH A SiLi DETECTOR.

9
Master's THESIS

Presented to the Faculty of the School of Engineering
of the Air Force Institute of Technology
Air University
in Partial Fulfillment of the
Requirements for the Degree of
Master of Science

15
✓✓ ARPA Order-1841

by

10
Charles E. Rowe B.S.M.E.
2Lt. USAF

Graduate Nuclear Engineering

11
March 1974

12
61p.

ACCESSION for	
NTIS	White Section <input checked="" type="checkbox"/>
DDC	Buff Section <input type="checkbox"/>
NAVJAG	<input type="checkbox"/>
ISICATV	<input type="checkbox"/>
BY	
DISTRIBUTION/AVAILABILITY CODES	
SPECIAL	
A	

Approved for public release and sale. Distribution unlimited.

1473
012 225

LB

Preface

This thesis was an attempt to portray six months of effort in the development of a new and untried detection system. The endeavor involved the creation of new equipment and techniques to support the effort. I hope the language of the report conveys as much information as possible without being too elementary.

There are too many people that I owe thanks to list them all here. But to my thesis advisers, Dr. George John and Dr. G. R. Hagee, I owe my first debt, the chance to do this work and all the help and suggestions offered by them. To the technicians in the Physics Department and their assistance I am grateful. To Mr. Wolfe and the personnel of the School Shop I am indebted for their efforts and support.

Finally, I owe the most to my parents, whose encouragement and understanding really made this all possible.

Charles E. Rowe

Contents

	Page
Preface	ii
List of Figures	v
List of Tables	vi
Abstract	vii
I. Introduction	1
II. Preliminary Considerations	6
Decay Spectrum of Xe^{131m}	6
Vapor Pressure of Solid Xenon	8
Sublimation Rate of Solid Xenon in a Vacuum	9
III. Equipment	13
Detector, Preamp and Amplifier	14
Multichannel Analyzer	14
Detection Chamber	14
Gas Handling Manifold	19
Equipment Set-up	20
IV. Experimental Procedure, Data Analysis and Results	23
Original Detection Chamber	23
Modified Detection Chamber	25
Exposure Loss and Handling Loss	25
Background	26
Xe^{131m} Spectrum and Resolution	26
Repeatability and Efficiency	28
Self Absorption	29
V. System Characteristics	32
VI. Discussion, Conclusions and Recommendations .	35
Bibliography	39
Appendix A: Pump Rate Determination	41
Appendix B: Inherent Loss	43
Appendix C: Effect of Deposition Profile	44
Appendix D: Minimum Activity	46

Contents

	Page
Appendix E: Gas Handling Manifold	49
Vita	52

List of Figures

Figure		Page
1	Xe ^{131m} Decay Scheme	6
2	Vapor Pressure of Solid Xenon vs Temperature . .	10
3	Detection System	15
4	Detection Chamber	16
5	Modified Detection Chamber	18
6	Gas Handling Manifold	19
7	Equipment Set-up	21
8	Grams Lost vs Exposure Time for Xenon Deposited as a Solid on an Area of 5.1 cm ² and Exposed to a Vacuum of 10 ⁻⁵ mmHg	24
9	Xe ^{131m} Spectrum	27
10	Xe ^{131m} X-ray Spectrum	27
11	Effect of Self Absorption of K-Internal Conversion Electron Peak of Xe ^{131m}	30
12	Relative Effect of Self Absorption as measured by the Ratio of Xe ^{131m} K-Internal Conversion Electron Peak Height to Tail for Different Masses of Xenon at 5.3 x 10 ⁴ DPM/std. cm ³	33
13	Xe ^{131m} Activity vs Counting Time Required for a Significance Level of 5%	34
14	Proposed Detection Chamber	37
15	Pump Rate Configuration	42
16	Gas Handling Manifold	50

List of Tables

Table		Page
I	Decay Spectrum of $\text{Xe}^{131\text{m}}$	8
II	Corrections to be Applied to the Podgurski-Davis Equation to Obtain the Vapor Pressure of Solid Xenon	10
III	Deposition Profile Data	44

QUANTATIVE ANALYSIS OF RADIOACTIVE
NOBLE GASES WITH A SiLi DETECTOR

I. INTRODUCTION

This thesis reports on the development of a system, which employs a cooled semiconductor detector, and on the assessment of the practicality of its use for the quantitative analysis of radioactive noble gases, specifically, the practicality of its use for the analysis of gas samples at low levels of radioactive concentration. The system under consideration employs a 300 mm² by 5 mm lithium drifted silicon (SiLi) detector maintained at liquid nitrogen temperature in a high vacuum environment. Analysis of the characteristics of the system is based on the detection of the xenon radionuclide Xe^{131m}, however, the results can be applied to the analysis of radioactive noble gases with cooled semiconductor devices in general.

The quantitative analysis of radioactive noble gases, and xenon in particular, has already been accomplished with the use of scintillation systems. Liquid scintillators have been used for some time in the analysis of xenon radionuclides because of their high efficiency for electrons and the high solubility of xenon in the aromatic hydrocarbons used in liquid scintillation systems (Ref 5:2077). The incorporation of xenon directly in the scintillator enhances the sensitivity for detection of electrons since the geometric losses and self absorption are eliminated. In addition, the dimensions of the container can be made sufficiently

large to insure the electrons expend all of their energy in the sensitive volume. Consequently, the intrinsic efficiency of liquid scintillators can approach 100% for electrons (Ref 5:2078). The intrinsic efficiency for electromagnetic radiation, however, is not as good because of the low absorption coefficients for low Z materials. Specifically, carbon has a photoelectric - mass absorption coefficient of $0.05 \text{ cm}^2/\text{gm}$ at 30 keV (Ref 15) which is close to the energy of xenon K x-rays.

The motivation for exploring the use of cooled semiconductor devices for the analysis of radioactive noble gases lies in the possibility of increased sensitivity due to their excellent resolution and high intrinsic efficiency. In a semiconductor system, the overall efficiency for electrons is primarily influenced by the geometric efficiency since the source is outside of the sensitive volume of the detector. There is no real problem with absorbing the total energy of an incident electron, however, since a depletion depth sufficient to completely stop the electrons of interest can be specified. With a 4π geometry, the intrinsic efficiency of the system for electrons can approach that available in scintillation systems. In addition, since the photoelectric - mass absorption coefficient for silicon is $1.17 \text{ cm}^2/\text{gm}$ at 30 keV (Ref 15), the intrinsic efficiency of a silicon semiconductor can be about twenty times that of liquid scintillators for xenon K x-rays.

The major advantage, if it can be capitalized on, of a cooled semiconductor over a liquid scintillation system is its

superior resolution. The resolution, in terms of full width at half maximum (FWHM), is proportional to the square root of the average energy required to produce an electron-hole pair in the detector (ϵ) times the Fano factor for the device (Ref 14). For scintillation systems, ϵ is about 500 eV/pair and the Fano factor is between 1/3 and 1/2 (Ref 14). For cooled silicon detectors, ϵ is 3.23 eV/pair (Ref 14) and the ultimate Fano factor is 0.05 (Ref 9:221). The theoretical FWHM of a silicon detector can, therefore, be from 1/31 to 1/39 that of scintillation systems. Since increasing the resolution increases the signal to noise ratio, a cooled silicon detector could, for the same time period and system efficiency, measure much lower activities than a liquid scintillation system.

If one is to take advantage of the high resolution of cooled semiconductor devices for electron detection, the degradation of resolution by absorption or self absorption must be minimized. In the system under consideration, which was nearing construction completion at the onset of this study, the original design called for the deposit of xenon as a solid in the immediate vicinity of the detector by freezing it on a cold finger at liquid nitrogen temperature. The degradation of resolution due to self absorption was to be minimized by depositing the xenon in a very thin layer. For proper operation the detector was to be cooled to liquid nitrogen temperature in a high vacuum environment maintained by Zeolite pellets. Exposure of a xenon sample, even in the solid state, to such an environment would cause sample loss by absorption

in the pellets at a rate determined by the sublimation rate of solid xenon and the pump rate of the system. To avoid this a mylar window was to isolate the sample from the Zeolite pellets. However, due to an error in the construction phase, the window was left out. The exposure-loss rate of xenon in this configuration was experimentally determined and, as expected, proved the configuration impractical for xenon analysis. The system was therefore modified to resemble the original design.

In the modified version of the detection system a thin mylar window, located between the xenon sample and the detector, isolates the sample from the pumping action of the Zeolite pellets. The exposure-loss rate of a xenon sample will theoretically be zero for such a configuration but should be experimentally verified. Another mode of sample loss which needs to be determined is the handling loss which can occur due to the physical configuration for transfer of samples into the system. Other factors or system characteristics which need to be considered are the effect of sample thickness on resolution degradation and the effect of the mylar window between the xenon and detector. In addition, the reproducibility of analysis, sensitivity of the system, and efficiency of the system for both xenon x-rays and electrons need to be determined.

The plan of the following chapters is as follows. Preliminary considerations are discussed in Chapter II. In Chapter III, a brief discussion of the equipment and equipment set-up is given. Chapter IV covers experimental

procedure, data analysis, and results. Chapter V presents the system characteristics established from experimental data and theoretical considerations. Discussions, conclusions, and recommendations for further work are presented in the final chapter, Chapter VI.

II. Preliminary Considerations

This chapter presents the decay spectrum of $\text{Xe}^{131\text{m}}$ and the vapor pressure of xenon at liquid nitrogen temperature. In addition, the sublimation rate of solid xenon in a high vacuum environment is calculated. These parameters are used throughout the study and are needed for the assessment of system characteristics.

Decay Spectrum of $\text{Xe}^{131\text{m}}$

The decay scheme of $\text{Xe}^{131\text{m}}$ is shown in Figure 1.

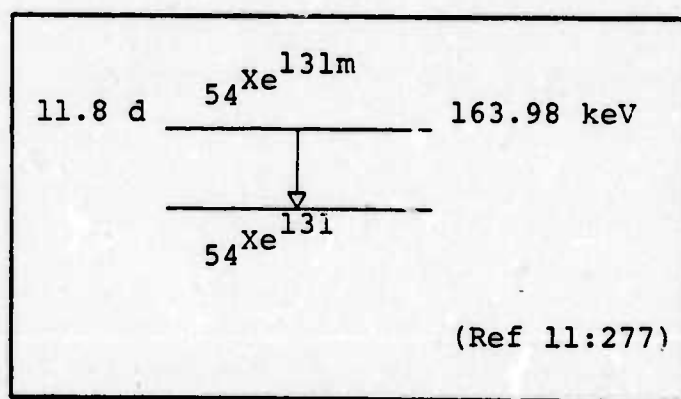


Figure 1. $\text{Xe}^{131\text{m}}$ Decay Scheme

To determine the spectrum produced by the decay of $\text{Xe}^{131\text{m}}$ the following parameters are needed:

- 1) $E_{\gamma} = 163.98 \text{ keV}$
- 2) $e_{\text{K}/\gamma} = 29, \quad \text{K/L} = 2.3$
- 3) Binding energy of Xe electrons: $\text{K} = 34.561 \text{ keV},$
 $\text{L} = 5.453 \text{ keV}$
- 4) Fluorescent yield $(\omega_{\text{K}}) = 0.87$
- 5) Energy of Xe K x-ray = 29.78 keV (Ref 10)

The number of 163.98 keV gamma rays and K or L internal conversion electrons per disintegration of $\text{Xe}^{131\text{m}}$ are calculated from the following relations:

$$\gamma/\text{dis} = \frac{\gamma}{\gamma + e_K + e_L}$$

$$e_K/\text{dis} = \frac{e_K}{\gamma + e_K + e_L}$$

$$e_L/\text{dis} = \frac{e_L}{\gamma + e_K + e_L}$$

The number of Xe K x-rays and Auger electrons per disintegration can then be determined with the relations:

$$\text{K x-rays/dis} = e_K/\text{dis} \times \omega_K$$

$$\text{Auger e/dis} = e_K/\text{dis} \times (1 - \omega_K)$$

The energies of the various decay modes can be calculated from the following:

$$E_{e_K} = E_\gamma - \text{B.E.}_K$$

$$E_{e_L} = E_\gamma - \text{B.E.}_L$$

$$E_{\text{Auger e}} = \text{B.E.}_K - 2 \times \text{B.E.}_L \quad (\text{Ref 3})$$

The type, energy, and relative abundance of the radiation emitted as the result of the decay of $\text{Xe}^{131\text{m}}$ are tabulated in Table I.

Table I
Decay Spectrum of $\text{Xe}^{131\text{m}}$

Type	Energy (keV)	Relative Abundance
$\text{Xe}^{131\text{m}} \gamma$	163.98	0.024 per $\text{Xe}^{131\text{m}}$ decay
$\text{Xe}^{131\text{m}} e_L$	158.4	0.296 per $\text{Xe}^{131\text{m}}$ decay
$\text{Xe}^{131\text{m}} e_K$	129.3	0.681 per $\text{Xe}^{131\text{m}}$ decay
Xe K x-rays	29.78	0.592 per $\text{Xe}^{131\text{m}}$ decay
Xe Auger e	23.70	0.0885 per $\text{Xe}^{131\text{m}}$ decay

Vapor Pressure of Solid Xenon

Throughout this study, xenon is transferred and isolated in the detection system by cryogenic pumping. Specifically, the sample is isolated in or on cold fingers by lowering the temperature of these areas to liquid nitrogen temperature. Liquid nitrogen, with a boiling point of 77.4°K, is cold enough to maintain xenon, with a melting point of 161.3°K, in the solid state (Ref 16). To determine the sublimation rate of solid xenon in a vacuum it is first necessary to ascertain its vapor pressure. This factor is also required in the evaluation of handling losses in the system and the determination of pumping rates.

In 1961 Podgurski and Davis proposed the following equation for the vapor pressure of xenon in the temperature range of 70 to 90°K (Ref 13:1397):

$$\text{Log}_{10} p = 8.044 - \frac{833.33}{T}$$

where

p = vapor pressure in mmHg

T = temperature in °K

In 1964 Gruther and Shorrock reviewed the equations available for xenon vapor pressure and compared them to the curve calculated from the calorimetric data of Clusius and Riccoboni (Ref 4:1084). Gruther and Shorrock concluded that the Clusius-Riccoboni vapor-pressure curve should be used for the vapor pressure of solid xenon with an estimated error of $\pm 2\%$ in the range of 70 to 161°K. The vapor pressure is most easily calculated by using the Podgurski-Davis equation in conjunction with the corrections provided by Gruther and Shorrock (Ref 4:1085). The corrections are given in Table II and a plot of the vapor pressure of xenon from 70 to 110°K is shown in Figure 2. From the plot it can be seen that the vapor pressure of xenon at 77.4°K is 1.9×10^{-3} mmHg.

Sublimation Rate of Solid Xenon in a Vacuum

The rate at which solid xenon will disperse in a high-vacuum system depends on whether or not the vacuum is maintained by pumping. If the sample is isolated from vacuum pumps, the dispersal rate is the same as the sublimation rate and the total amount of material lost from the solid is determined by its vapor pressure and the volume of the vacuum container. If the sample is not isolated, the dispersal rate will be determined by both the sublimation rate and the pump rate. The total material lost in this case, is limited only by the time of exposure. In either case, the sublimation rate of xenon needs to be determined.

According to Langmuir, if the temperature of a substance is lowered beyond the point where the vapor pressure

Table II

Corrections to be Applied to the Podgurski-Davis Equation to
Obtain the Vapor Pressure of Solid Xenon

$T(^{\circ}\text{K})$	$\text{Log}_{10} P$
70	PD + 0.0028
80	PD + 0.0000
90	PD - 0.0072
100	PD - 0.0164
110	PD - 0.0275

(Ref 4:1085)

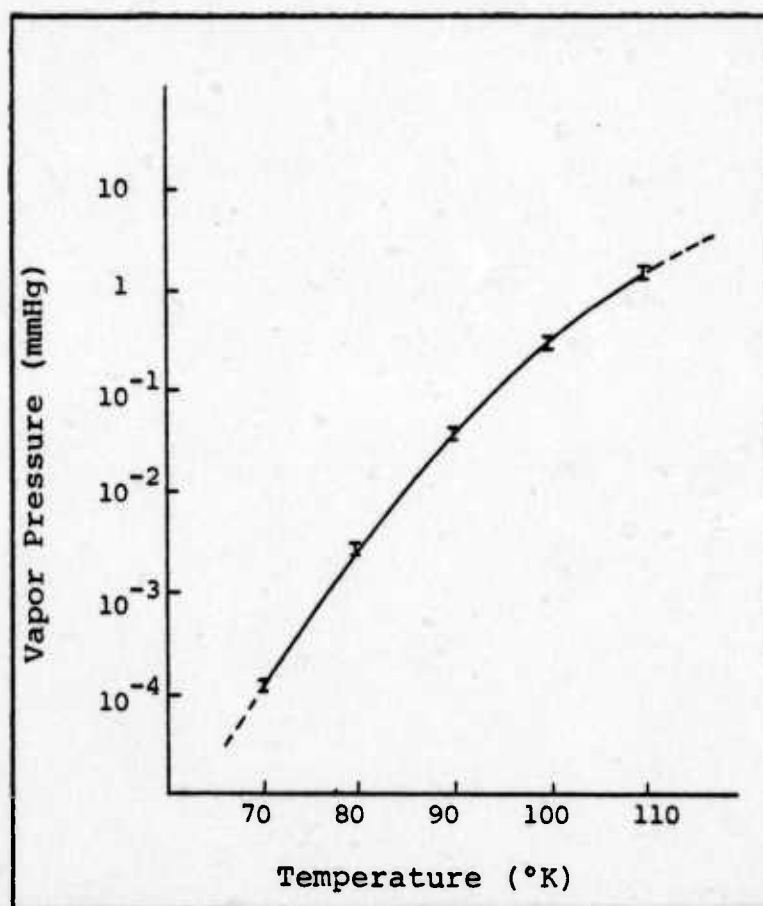


Figure 2. Vapor Pressure of Solid Xenon
vs Temperature

is a millimeter of mercury, then the rate of evaporation or sublimation can be considered independent of the presence of the vapor. The evaporation rate in a high vacuum will be identical to the evaporation rate in the presence of the saturated vapor (Ref 10:330). Since the vapor pressure of xenon at liquid nitrogen temperature is only 1.9×10^{-3} mmHg, it meets Langmuir's criteria. Then for a solid in equilibrium with its saturated vapor:

$$\mu = \alpha v \quad (1)$$

where μ = rate at which molecules sublime from surface

α = condensation coefficient

v = number of molecules of a gas at rest as a whole that strike unit area per unit time

The condensation coefficient or "sticking" coefficient is the ratio of the number of molecules which strike the surface to the number of molecules which stick to the surface. Taking the condensation coefficient as 1 will give the most conservative, or slowest, sublimation rate. We then have:

$$\mu = v = \frac{1}{4} n v_a \quad (\text{Ref 1:18}) \quad (2)$$

where n = the number of molecules per cubic cm

v_a = the arithmetic average velocity of molecules at a given temperature

In terms of temperature and pressure:

$$n = 0.656 \times 10^{18} \frac{\text{Pmm}}{\text{T}} \text{ cm}^{-3} \quad (3)$$

$$v_a = 14,551 \left(\frac{\text{T}}{\text{M}} \right)^{1/2} \text{ cm/sec} \quad (\text{Ref 1}) \quad (4)$$

Combining equations 2, 3, and 5 leads to:

$$\mu = 3.5126 \times 10^{22} \frac{P_{\text{mm}}}{T^{1/2} M^{1/2}} \text{ molecules/cm}^2\text{-sec} \quad (5)$$

To obtain results in grams:

$$G = \frac{\mu}{N_a} M \quad (6)$$

$$G = 0.05831 P_{\text{mm}} \left(\frac{M}{T}\right)^{1/2} \text{ grams/cm}^2\text{-sec} \quad (7)$$

For xenon at liquid nitrogen temperature exposed to a vacuum less than its vapor pressure (1.9×10^{-3} mmHg) the sublimation rate is:

$$G = 1.444 \times 10^{-4} \text{ grams/cm}^2\text{-sec}$$

III. Equipment

This chapter describes the equipment used in the experimental work, including the detector, preamp, amplifier, multichannel analyzer, detection chamber, and gas handling manifold. The equipment set-up is also described and a brief description of the operation is included.

Detector, Preamp, and Amplifier

The lithium-drifted silicon detector used throughout this study was manufactured by the KeVex Corporation of California. The detector, which has an active area of 300 mm^2 and a sensitive depth of 5 mm, must be operated at liquid nitrogen temperature in a vacuum of at least 10^{-4} mmHg . The detector cannot be temperature cycled more than 25 times nor left at room temperature for more than 100 hours without suffering degradation in resolution. The manufacturer specified a resolution, in terms of FWHM, of 265 eV at 5.9 keV (Ref 7) and the sensitive depth of the detector is sufficient to completely stop 2.7 meV electrons (Ref 12).

The preamp and linear amplifier used in this study were also manufactured by the KeVex Corporation. The preamp and amplifier were designed for low noise operation, in particular, the first stage of the preamp, a field-effect transistor (FET), is an integral part of the detector assembly. This helps to reduce electronic noise by shortening the lead length between the detector and FET.

The principle of operation is as follows. An electron entering the sensitive region of the detector produces

electron-hole pairs. For silicon, 3.23 eV of energy is required to produce each electron-hole pair. Photons entering the sensitive region can transfer their energy to charged particles in the detector by the photoelectric effect, Compton scattering, or pair production. The charged particles can then produce electron-hole pairs. The charge is collected under the influence of a -300 to -1000 volt bias and converted to a voltage pulse by the charge sensitive preamp. The pulse is then amplified by the linear amplifier for analysis by a multichannel analyzer (MCA). Since the voltage is proportional to the collected charge and the charge is proportional to the energy of the incident radiation, the channel in the MCA in which the voltage pulse is stored is proportional to the energy of the incident radiation expended in the detector.

Multichannel Analyzer

The multichannel analyzer used in this study was a Nuclear Data Model 2200 with a 4096 channel memory. It has the capability of storing four 1024 channel spectra in its memory and, after storage, any of these spectra can be overlapped on the MCA for comparison. The MCA was linked to a Precision Equipment Company tape deck, a teletype printer, and a plotter. Data could be stored on magnetic tape and either printed out on the teletype or plotted on the plotter.

Detection Chamber

The detection chamber as originally constructed is shown in Figure 3 and Figure 4. The chamber is constructed

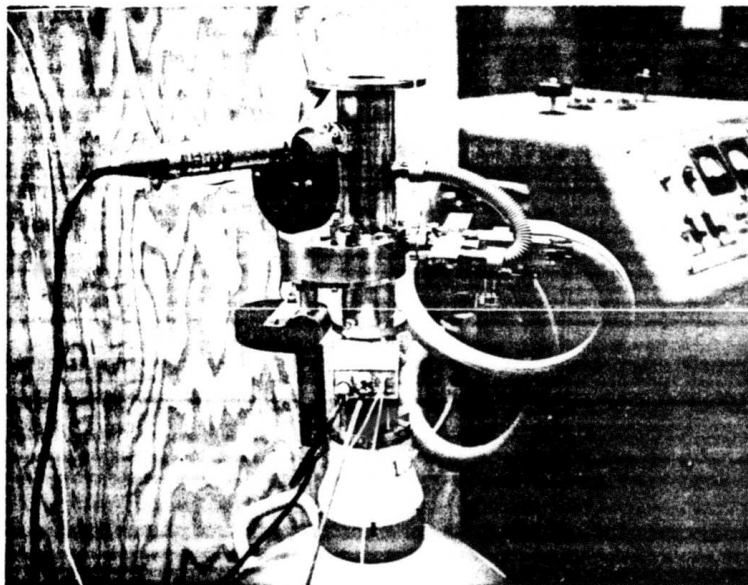
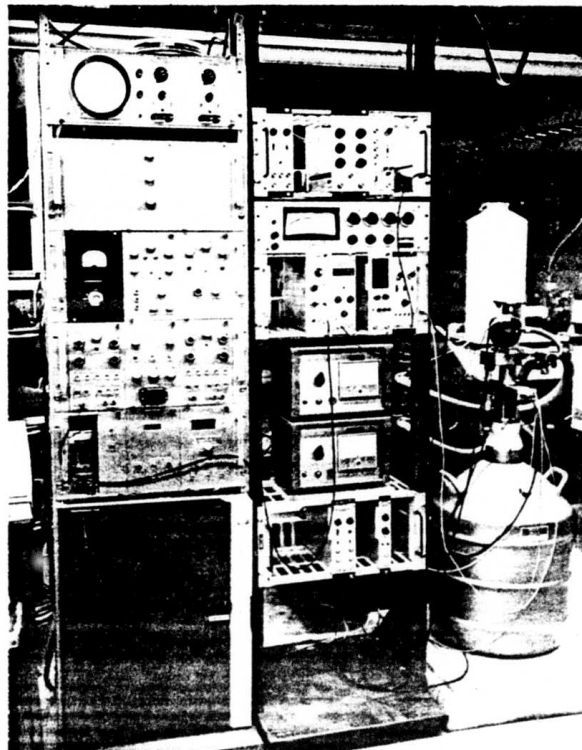


Figure 3. Detection System.

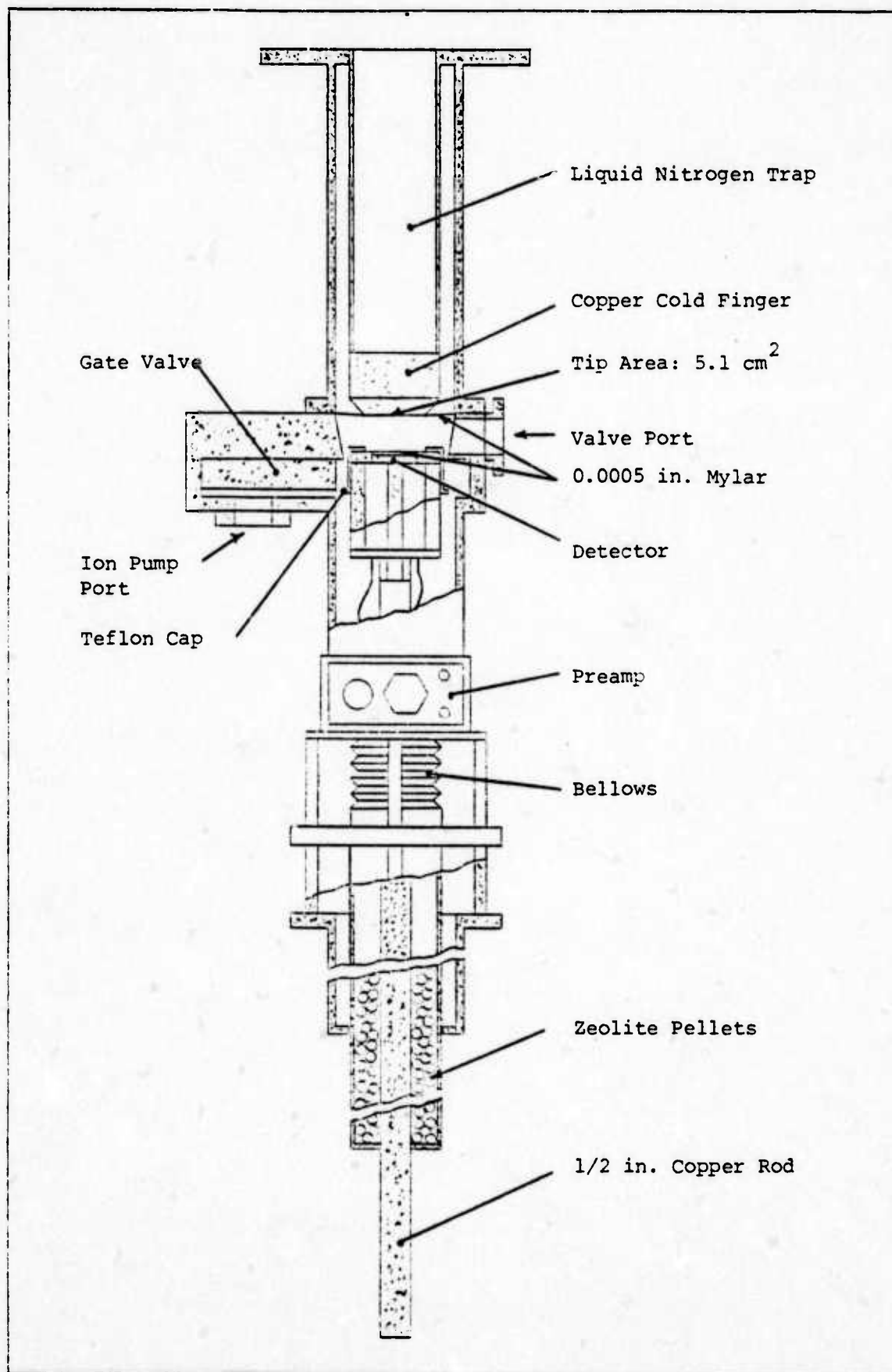


Figure 4. Detection Chamber

primarily of stainless steel and has a valving arrangement to allow introduction of xenon samples. Attachment of a vacuum pump to the valving arrangement allows evacuation of break-seal tubes when a sample is to be introduced or removed from the system. Within the chamber, the detector is mounted on a copper rod which, when the system is set in a liquid nitrogen cryostat, cools the detector assembly. The vacuum of the chamber is maintained at 10^{-5} to 10^{-6} mmHg by the use of ion pumps and Zeolite pellets. A bellows arrangement allows positioning of the detector with respect to the site of sample deposition and a gate valve can be used to isolate the detector from the remainder of the system.

In the original construction configuration, a mylar sheet stretched across the cold finger was the site of xenon deposition. The 0.0005 inch mylar sheet was bonded to the outer shell of the liquid nitrogen trap with RTV. The copper tip of the cold finger extends 0.010 inch past the bond plane to insure contact between the surface of the copper tip and the mylar sheet.

In the modified version of the system, shown in Figure 5, a special chamber was added to isolate the sample from the rest of the system. The stainless steel chamber is silver soldered to the copper cold finger and a 0.0005 inch mylar window is bonded to the chamber flange with Dow Corning 93-004 Aerospace Sealant. A short stainless steel tube is silver soldered to the chamber and attaches to a teflon tube with a flange at one end to provide a vacuum tight seal by use of

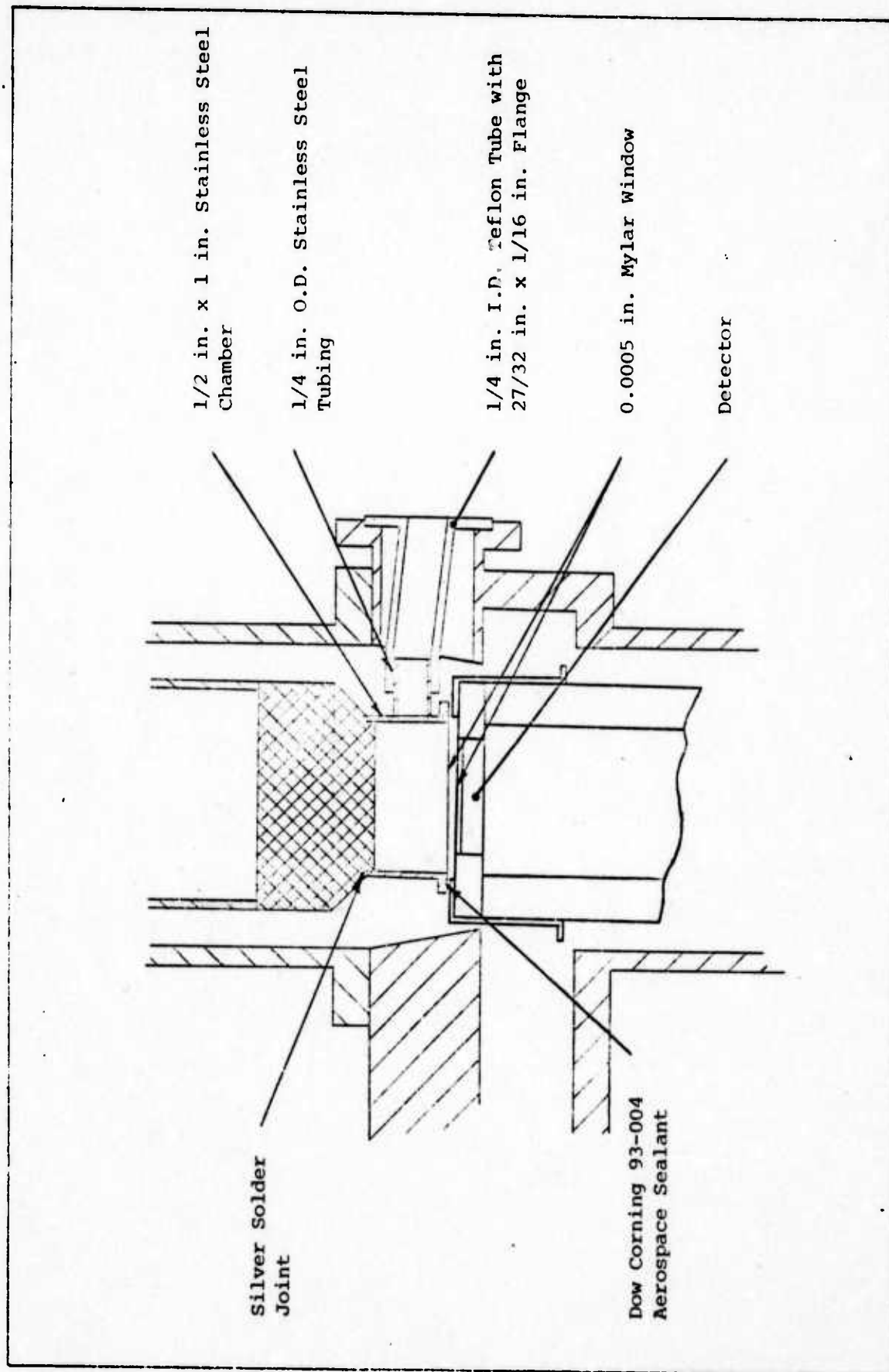


Figure 5. Modified Detection Chamber

the knife-edges of the valve system flanges. Via the valve system and the teflon tube, a sample can be introduced into the sample chamber and remain isolated from the vacuum of the detection chamber.

Gas-Handling Manifold

A gas-handling manifold was designed and built to provide the capability of precise sample-mass measurement. In addition, the gas handling manifold provides the means for dilution, combination, or division of gas samples as required for the evaluation of the detection system. The manifold, shown in Figure 6, is constructed with stainless steel and uses Nupro valves with Penton seals and polyethelene swage-lock fittings. Sections of the manifold are volume calibrated

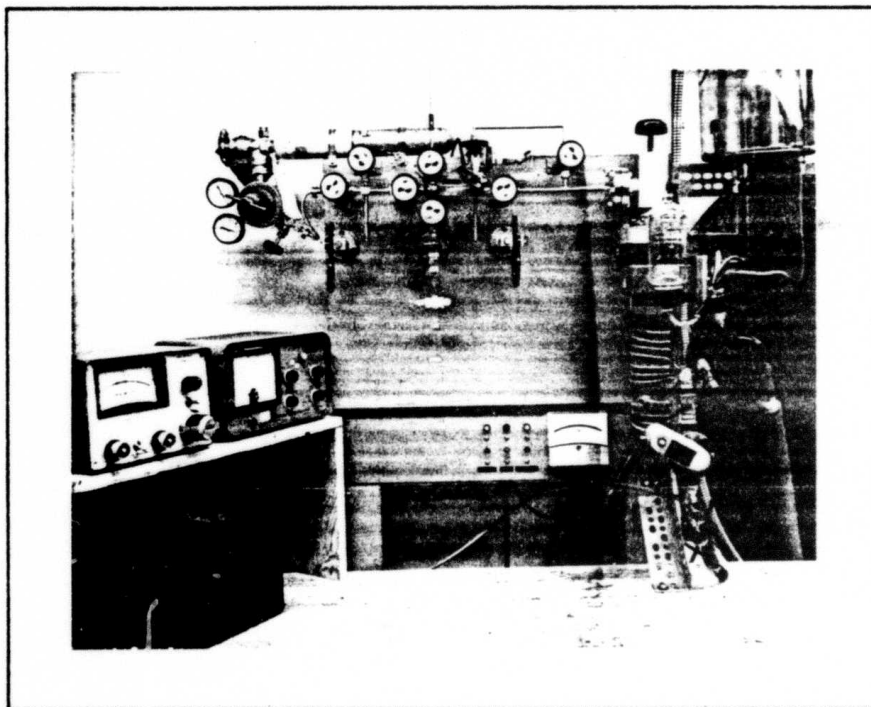


Figure 6. Gas Handling Manifold

and can be used in conjunction with a capacitive pressure transducer for precise sample-mass determination. The use of a liquid nitrogen trap together with a diffusion pump allows evacuation of the manifold to 10^{-7} mmHg. Further information on the gas handling manifold is presented in Appendix E.

Equipment Set-up

A block diagram of the system set-up is presented in Figure 7. A brief description of the procedure for sample analysis is as follows. The sample is first introduced into the gas handling manifold if the sample is to be measured, diluted, or only a portion used. The sample is then transferred from the gas handling manifold to the detection system by freezing it in a break-seal tube and sealing the tube with a torch. The sealed tube is removed from the gas handling manifold, connected to the detection system, and the volume between the break-seal and the introduction valve evacuated. The gas in the tube is then condensed with liquid nitrogen and, with the detector isolated by the gate valve, the liquid nitrogen trap in the detection chamber is filled, cooling the copper cold finger. The seal in the break-seal tube is broken and the tube warmed up to room temperature. As the tube warms up, the gas transfers and freezes onto the mylar sheet or into the sample chamber depending on the configuration used. The gate valve is then opened, the ion pumps turned off, and the detector positioned close to the sample before applying bias to the detector. As the sample spectrum is analyzed, the

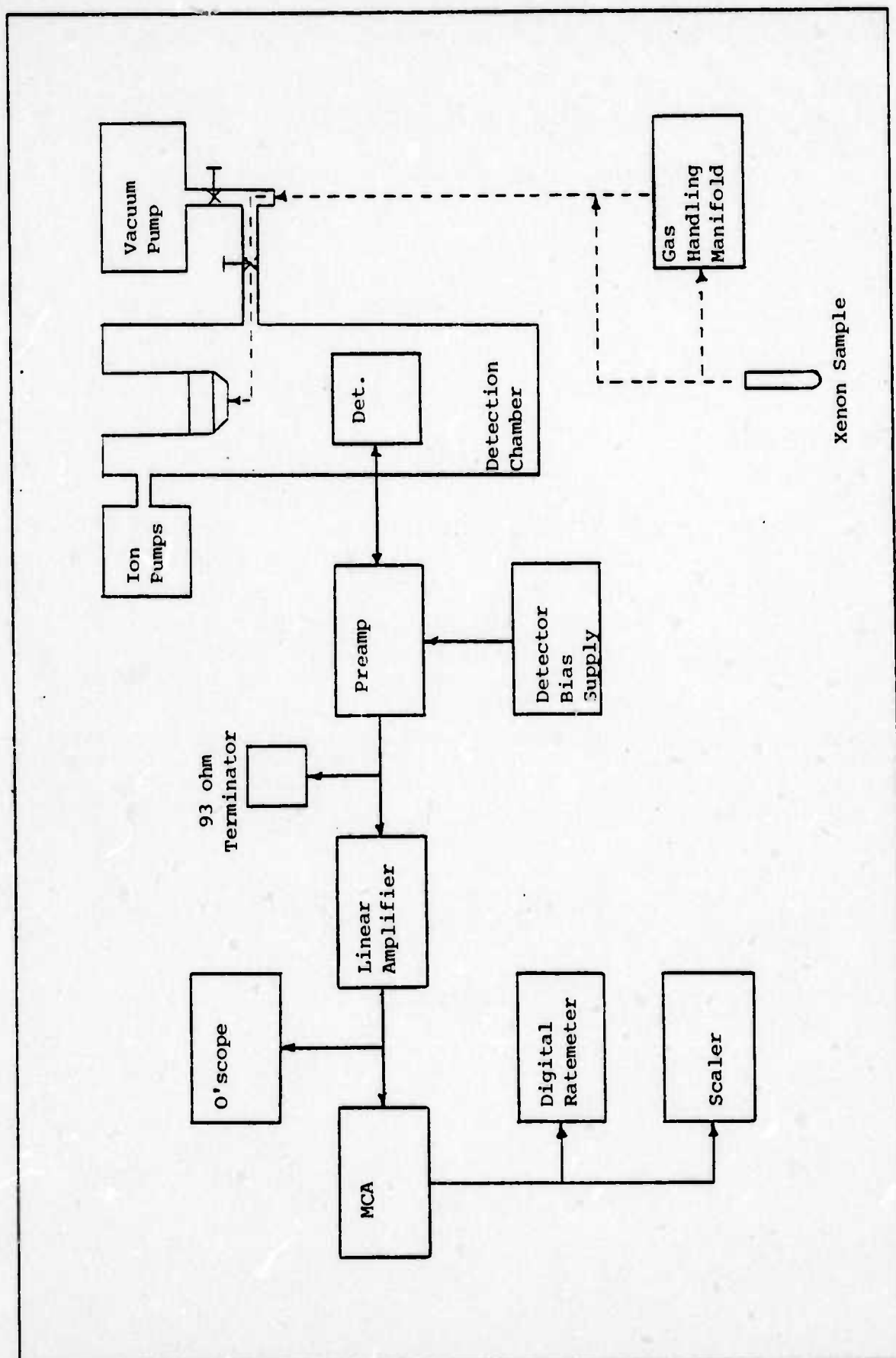


Figure 7. Equipment Set-up

GNE/PH/74-8

digital ratemeter indicates live time counts per second and the total counts for the run are accumulated by the scaler. To remove the sample after analysis, the process is simply reversed.

IV. Experimental Procedure, Data Analysis, and Results

This chapter details the experimental procedure followed for determination of system parameters. The data obtained is analyzed and the results presented.

Original Detection Chamber

From analysis of the detection chamber, as it was originally constructed, it appeared possible that a xenon sample frozen onto the mylar sheet could be lost at the rate of sublimation, 1.444×10^{-4} gm/cm²-sec. A cm³ of xenon at standard temperature and pressure deposited on the cold finger area of 5.1 cm² would, at this rate, disperse in less than 8 seconds. The actual loss rate was determined by two experimental methods. The results of these experiments, the sublimation rate, and a pump rate determined theoretically are shown in Figure 8. All of the curves are based on an exposure area of 5.1 cm².

In the first experimental method, the detection chamber configuration was approximated in the gas handling manifold by freezing xenon in a cold finger such that the area of deposition equaled that in the detection chamber. The solid xenon was exposed for half-hour periods to a vacuum of 10^{-5} mmHg maintained by the vacuum pump of the gas handling manifold. At the end of each half hour, the xenon was allowed to thaw and the pressure of the gas measured. The xenon remaining was then refrozen and the process repeated. From the change in pressure between successive measurements the mass lost during the period of exposure was computed.

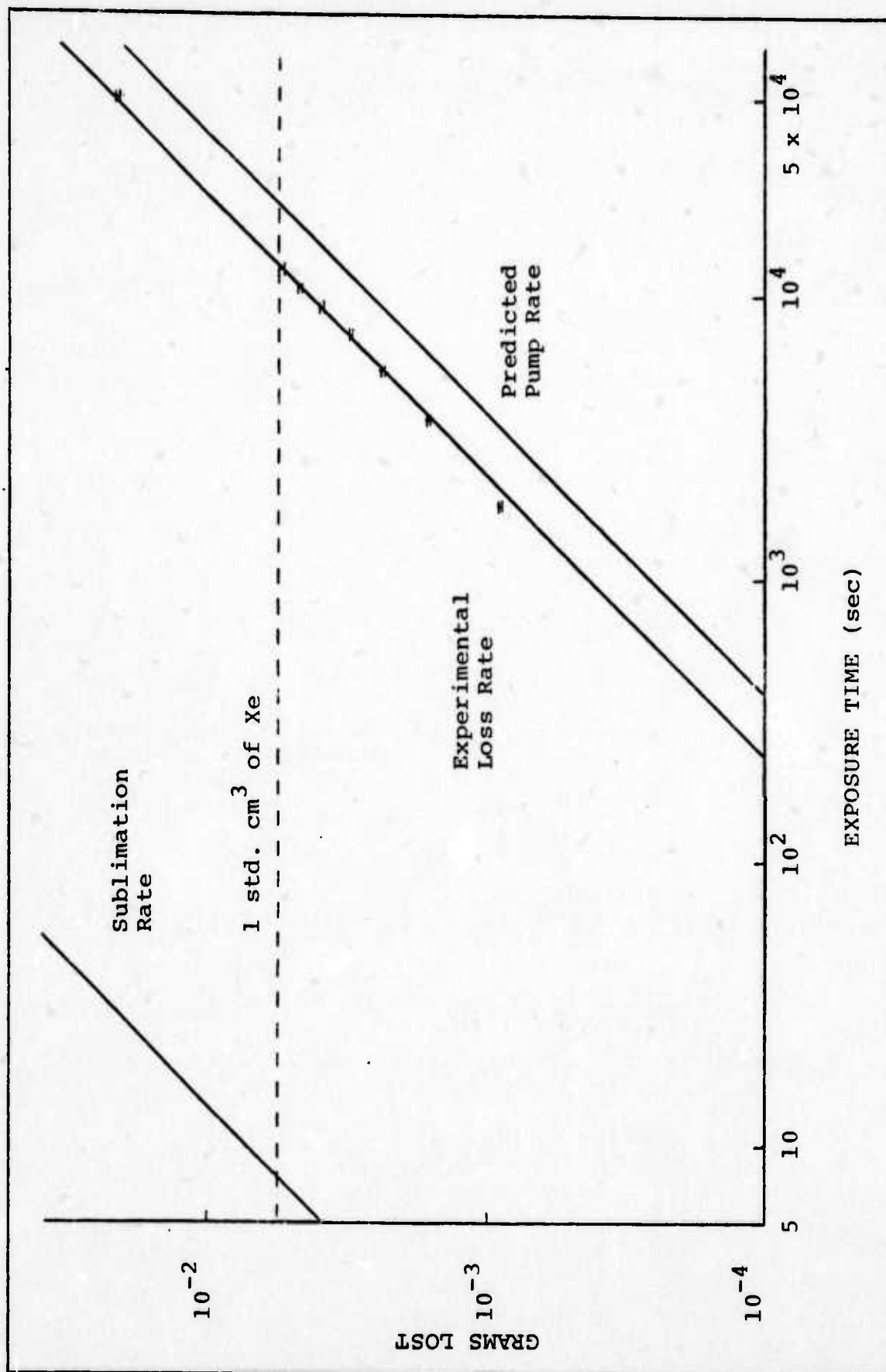


Figure 8. Grams Lost vs Exposure Time for Xenon Deposited as a Solid on an Area of 5.1 cm² and Exposed to a Vacuum of 10⁻⁵ mmHg.

The second method consisted of introducing a sample of known mass into the detection chamber, freezing it onto the mylar sheet, and exposing it to a vacuum of 10^{-5} mmHg maintained by the Zeolite pellets. After an exposure of 14 hours the sample was removed and its mass redetermined using the gas handling manifold. The difference between the initial and final mass measurements indicated that $2.16 \pm .06 \times 10^{-2}$ gm of xenon were lost during the period of exposure.

The experimentally determined loss rate, $4.3 \pm .1 \times 10^{-7}$ gm/sec, agrees reasonably well with the pump rate predicted from a model of the situation (see Appendix A). At this rate, a standard cm^3 of xenon would be removed in less than three hours. Although orders of magnitude less severe than the sublimation rate, the loss rate is far too fast for practical application of this configuration. For this reason the detection chamber was modified as described in the Equipment section.

Modified Detection Chamber

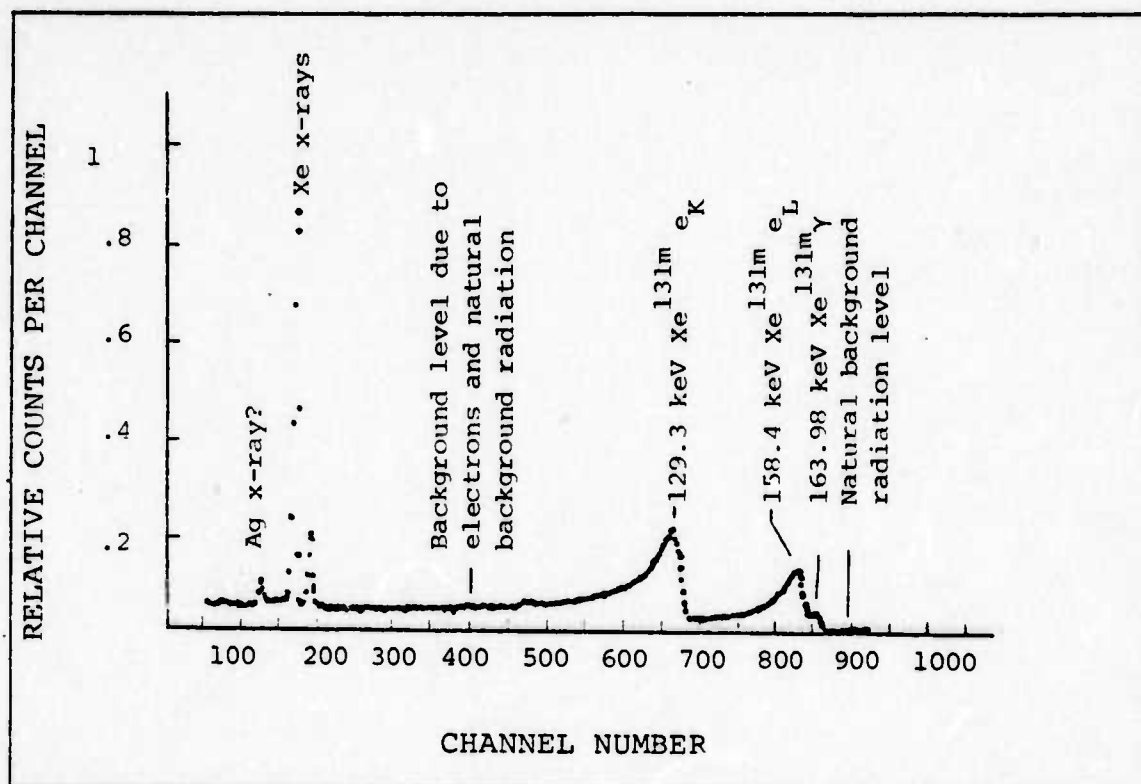
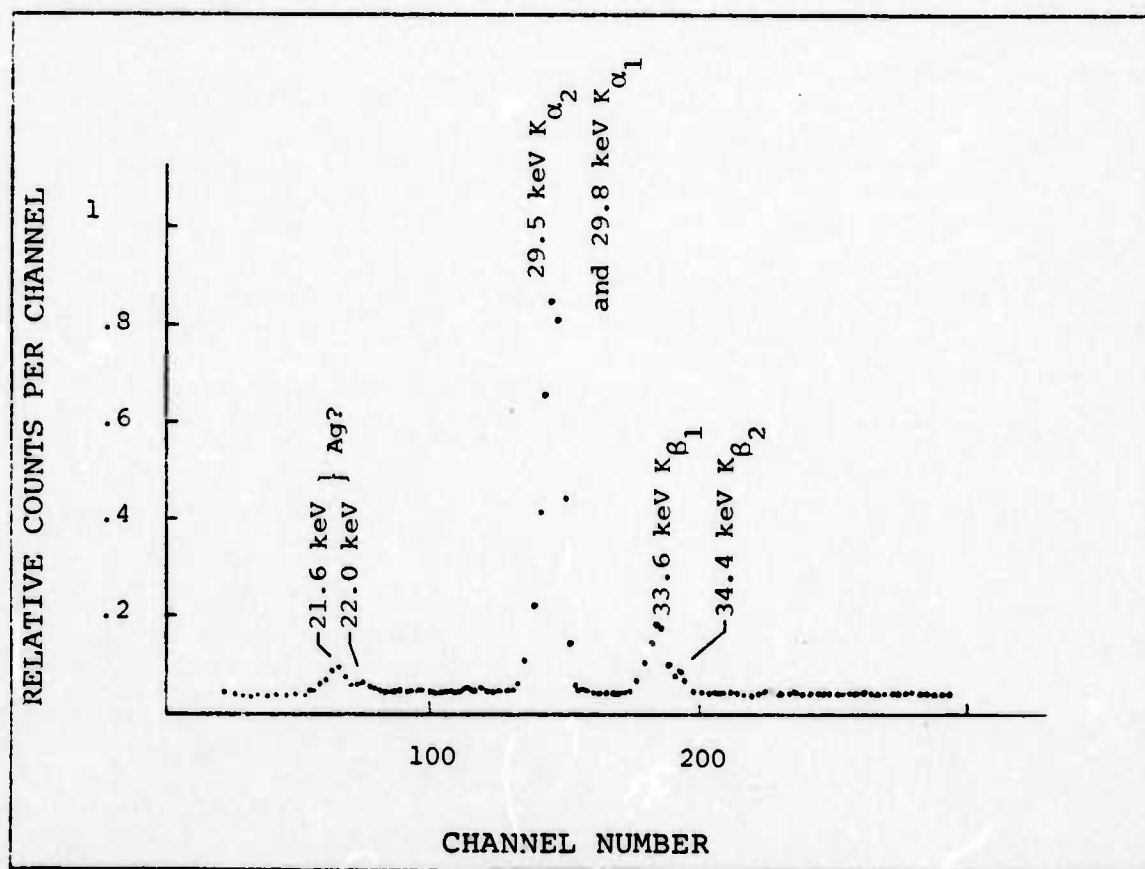
Exposure Loss and Handling Loss. In the modified version of the detection system, xenon samples are isolated from the pumping action of the Zeolite pellets by a mylar window. The exposure loss for a sample should, if there are no leaks in the system, be zero. To determine whether or not there is an exposure loss, a sample of xenon was introduced into the gas handling manifold and its mass determined. The sample was then transferred to the detection system and frozen in the sample chamber. This status was maintained for 14 hours, then the

sample was removed and its mass redetermined. Within the precision of gas-handling-manifold measurements, there was no change in the sample mass.

The minimum change in a xenon sample which can be measured with the gas handling manifold is 9.7×10^{-6} gm. Assuming the worst possible case for these experiments leads to an exposure loss of 1.4×10^{-6} gm/hour and a handling loss of 9.7×10^{-7} gm/cycle.

Background. Background radiation was measured with the system configured as for a sample analysis. Overnight background runs of 40 ksec were stored on the MCA and the total counts for the run stored on the scaler using the SCA output terminal of the MCA. Background runs showed no significant peaks and an even distribution over the entire spectrum. The average background radiation level was 0.07 CPM/keV from 8 to 240 keV.

Xe^{131m} Spectrum and Resolution. A Xe^{131m} spectrum typical of those obtained during this study is shown in Figures 9 and 10. The low energy tailing of the internal conversion peaks due to self absorption and absorption by the mylar window is evident in Figure 9 which shows the entire spectrum of Xe^{131m} from 8 to 180 keV. The count level due to natural radiation background can be seen at the high end of the spectrum, and the background level from the internal conversion electrons, due primarily to scatter in the detector, can be seen between the internal conversion electron peaks and the x-ray peaks. Figure 10 is an expanded view of the Xe^{131m} K x-rays and discloses the presence of peaks

Figure 9. $\text{Xe}^{131\text{m}}$ Spectrum.Figure 10. $\text{Xe}^{131\text{m}}$ X-ray Spectrum

at 21.6 keV and 22.0 keV which may be Ag x-rays.

The resolution shown in the figures is typical of the system, specifically, 0.749 keV at 33.6 keV. The initial resolution of the system was somewhat better than this, however, due to circumstances the detector had to be temperature cycled several times and a slight degradation of system resolution was introduced by each cycle.

Repeatability and Efficiency. A visual inspection of xenon deposited in the sample chamber of the modified detection system disclosed a variation in deposition profile with time. Xenon deposited in the chamber immediately after filling the liquid nitrogen trap would deposit as a spot on the center of the cold finger tip. As time went on, the temperature of the stainless steel walls of the chamber became colder and the xenon deposit redistributed itself until it covered both the cold finger tip and the walls of the chamber. Finally, after the chamber had been cooled for about a half hour, the deposit covered the cold finger tip, the walls of the chamber, and a portion of the mylar window. An area of concern was what effect these variations in xenon deposition profiles would have on the repeatability of measurements. To determine if there is an effect, a series of twenty measurements was obtained from a single radioactive sample that was cycled between each measurement. The raw data and method of analysis is presented in Appendix C. Since the counting data does not follow the expected Poisson distribution, it is concluded that differences in deposition profiles do introduce significant statistical variations. The repeatability of the measurements, as determined

in the appendix for the number of counts in the K x-ray peaks, is $\pm 2\%$ for 5506 counts.

The sample used in the above experiment was from a calibrated source which permitted the computation of efficiency from the known activity of the sample and the average count rate of the data. The number of counts produced by internal conversion electrons in the electron peaks plus tailing was determined from:

$$N_{\text{ICE}} = N_{\text{Total}} - N_{\text{x-ray}} - N_{\gamma} - N_{\text{nbg}} \quad (8)$$

where

N_{ICE} = total counts for internal conversion electrons

N_{Total} = total counts in entire spectrum

$N_{\text{x-ray}}$ = total counts in x-ray peaks.

N_{γ} = counts in gamma peak

N_{nbg} = counts from natural radiation background

The efficiencies determined were $3.0 \pm .4\%$ for xenon K x-rays and $14 \pm 2\%$ for $\text{Xe}^{131\text{m}}$ internal conversion electrons.

Self Absorption. The effect of self absorption of internal conversion electrons can be seen in Figure 11 which shows the K internal conversion electron peak of $\text{Xe}^{131\text{m}}$. The top spectrum was obtained with a $\text{Xe}^{131\text{m}}$ sample containing a total of 1.09×10^{-2} gm of xenon at a radioactive concentration of 12.8×10^4 DMP/std. cm^3 . The bottom spectrum was obtained with 8.27×10^{-4} gm of xenon in the sample at the same concentration. Both spectra have the same total count under the peak plus tailing at the low energy edge of the peak. To find the relative effect of self absorption with variation in total mass of xenon, several samples containing different masses of

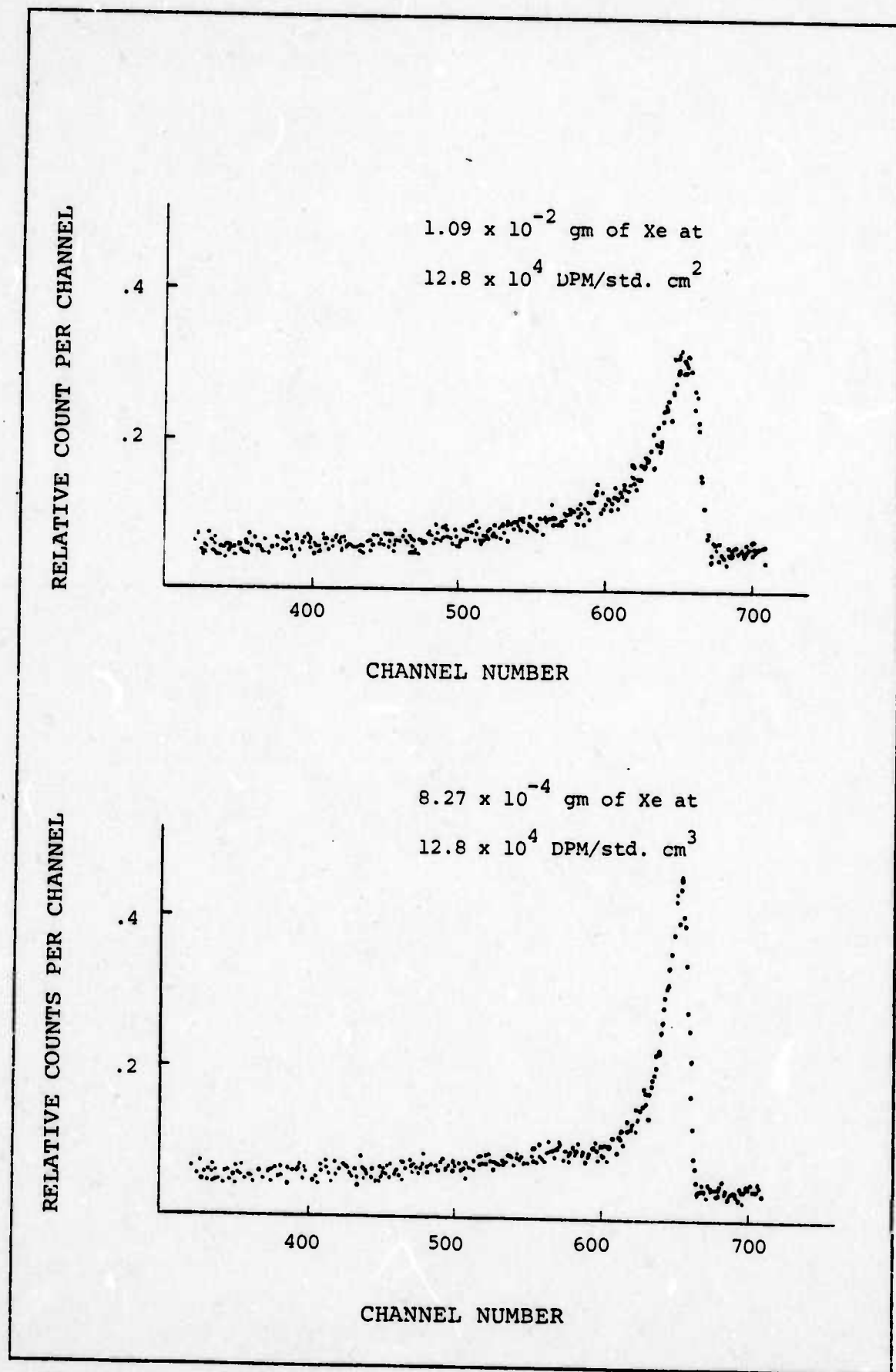


Figure 11. Effect of Self Absorption on K-Internal Conversion Electron Peak of $\text{Xe}^{131\text{m}}$.

xenon were counted until the same total counts were reached. All samples were from a source of known radioactive concentration. The results are shown in Figure 12 in the section on System Characteristics. The parameter of comparison is the height of the K internal conversion electron peak relative to its low-energy tailing background.

V. System Characteristics

The purpose of the various experiments and theoretical calculations performed in this study was to establish the characteristics of the detection system. For the two configurations considered, the following parameters were established.

Original Detection Chamber

Exposure Loss $1.55 \pm 0.03 \times 10^{-3}$ gm of Xe/hour

Modified Detection Chamber

Exposure Loss $< 1.4 \times 10^{-6}$ gm of Xe/hour

Handling Loss $< 9.7 \times 10^{-7}$ gm of Xe/cycle

Inherent Loss $\sim 6 \times 10^{-7}$ gm of Xe (see Appendix B)

Resolution 0.749 keV FWHM at 33.6 keV

Repeatability $\pm 2\%$ at 5506 counts for the K x-ray peaks (see Appendix C)

Background 0.07 CPM/keV from 8 to 240 keV

K x-ray Eff. $3.0 \pm .4\%$

ICe Eff. $14 \pm .2\%$

Self Absorption .. Figure 12

Minimum Activity . Figure 13 (see Appendix D)

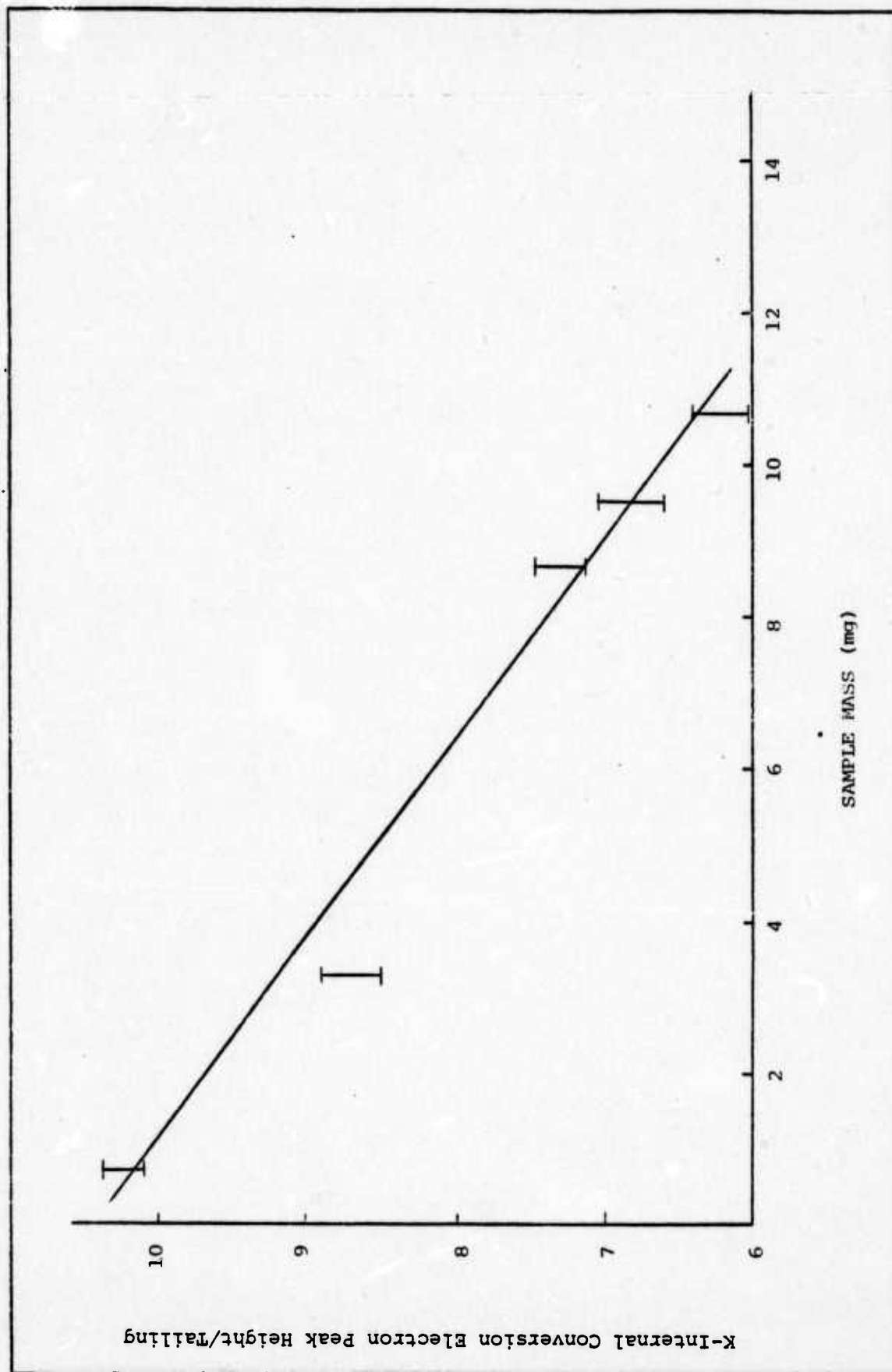


Figure 12. Relative Effect of Self Absorption as Measured by the Ratio of $\text{Xe}^{131\text{m}}$ K-Internal Conversion Electron Peak Height to Tailing for Different Masses of Xenon at 5.3×10^4 DPM/std. cm^3 .

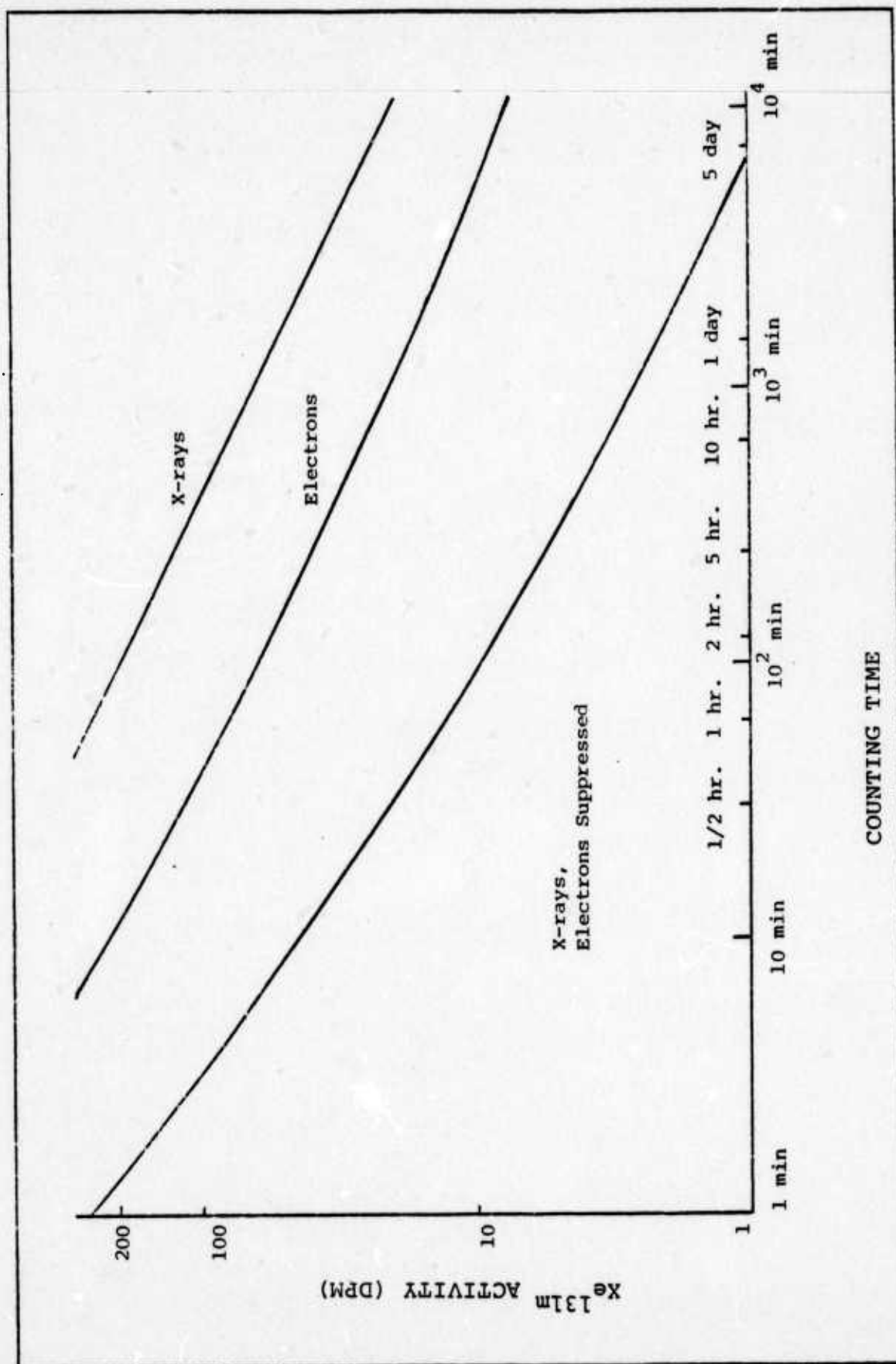


Figure 13. $\text{Xe}^{131\text{m}}$ Activity vs Counting Time Required for a Significance Level of 5%

VI. Discussion, Conclusions, and Recommendations

The purpose of this study was to develop a system which employs a cooled SiLi detector, and to assess the practicality of its use for the quantitative analysis of radioactive noble gases, particularly, the analysis of low-activity samples.

Based on theoretical considerations and experimental data the system as originally constructed was proven impractical due to the excessive sample-loss rate. The modified version shows promise, but further analysis is needed. Specifically, in-depth analysis of electron absorption and repeatability are required.

If repeatability can be established, the system as it stands could be used for the quantitative analysis of single noble gas radionuclides by either x-ray spectroscopy or internal conversion electron detection. In a ten-hour counting period, a significance level of 5% could be established for a $\text{Xe}^{131\text{m}}$ sample activity of about 25 DPM by internal conversion electron detection or about 90 DPM by x-ray spectroscopy. The required activity for other radionuclides would vary, of course, with the decay characteristics of the radionuclide. Quantitative analysis of mixed samples could be accomplished with x-ray spectroscopy, but would be extremely difficult by internal conversion electron detection due to the degradation of electron peaks.

It is strongly recommended that further work in this area be pursued. The hardware and software necessary for further analysis is available and in proven working condition.

Further analysis of the existing system could therefore be accomplished without difficulty. It is, however, recommended that certain modifications to improve the system and facilitate analysis be first considered.

The modification shown in Figure 14 would not involve extensive reconstruction and would improve the system as follows. The area of sample deposition would be much better defined and therefore reduce the effect of variation in deposition profiles. The improved geometry would increase the geometric factor and therefore the efficiency. The inherent loss would be reduced by the decrease in sample-chamber volume. Since the detector would be completely isolated, the protective mylar sheet across the face could be removed and removal of this absorber would decrease the degradation of the electron peaks. The detection chamber would be coupled directly to the gas handling manifold, eliminating the clumsy and time-consuming process of transfer by break-seal tubes.

The above factors would certainly lead to improved efficiency and hence, a reduction in required counting time for a given activity. In addition, the internal conversion peaks may become well enough defined to allow their use for the quantitative analysis of mixed samples.

Other configurations are possible, but may depend on unexplored factors. For example, if a vacuum seal could be established between the face of the detector and the remainder of the system, the sample could be deposited directly on the detector face. Removal of the sample would then

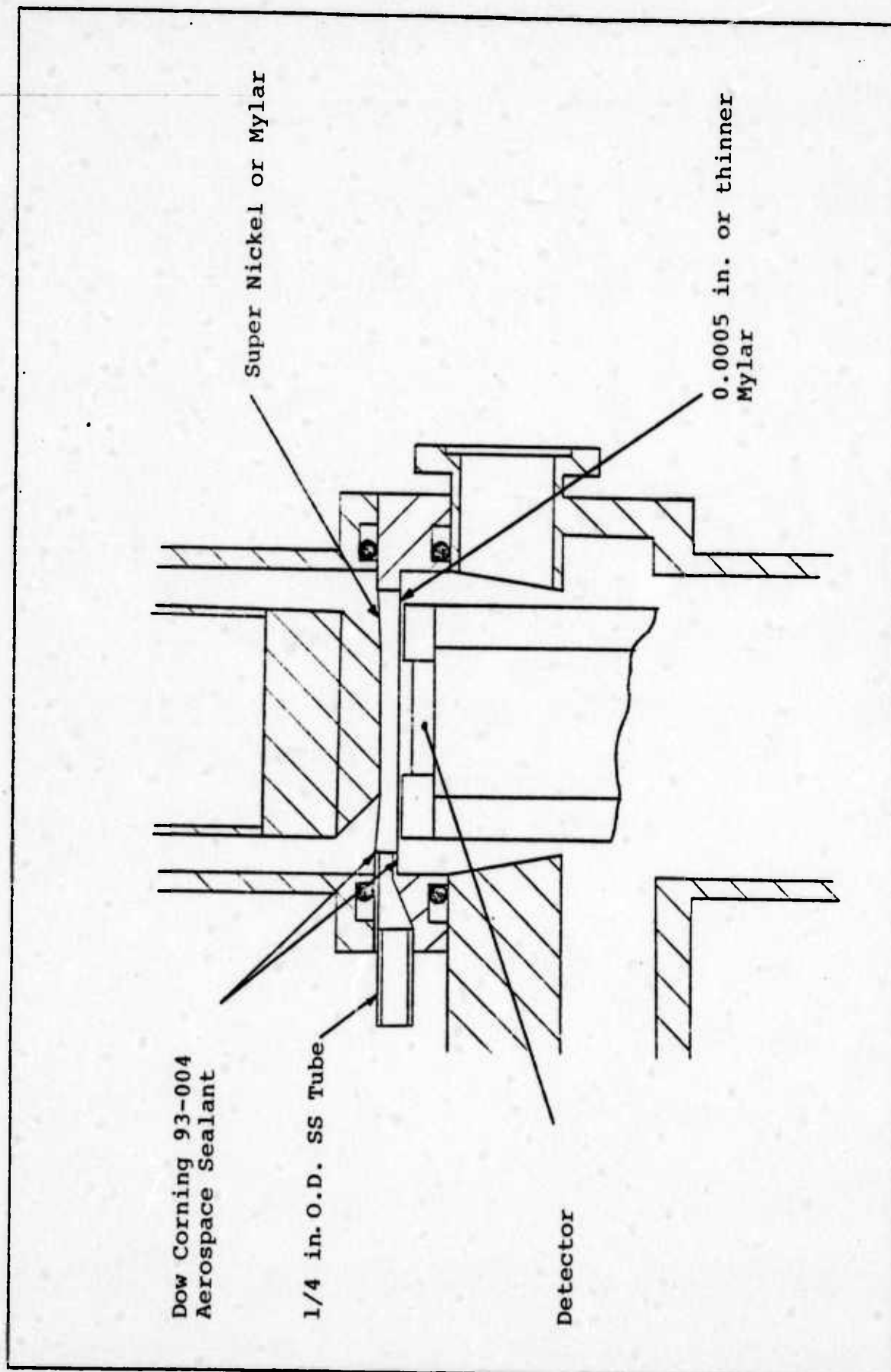


Figure 14. Proposed Detection Chamber

require cryogenic pumping at a temperature lower than that of liquid nitrogen.

Another possibility for consideration is using the system for x-ray spectroscopy and eliminating the internal conversion electrons with an absorber. If this could be accomplished in the present system the improvement in minimum detection level would be that shown by the "x-ray, electrons suppressed" curve in Figure 13. As shown on the curve, a significance level of 5% could be established for a $\text{Xe}^{131\text{m}}$ sample activity of 3 DPM in a counting period of 10 hours. In addition, if the system were geometrically optimized for x-ray detection, a geometric factor of 2π could be approached, improving the present efficiency by about a factor of three.

The potentials of this system for the quantitative analysis of radioactive noble gases can be improved. It is therefore urged that further analysis be performed and further modifications and improvements be explored.

Bibliography

1. Dushman, S. Scientific Foundations of Vacuum Techniques. (Second Edition) New York: John Wiley and Sons, Inc., 1962.
2. Emery, J. F., et al. "Half-Lives of Radionuclides-IV." Nuclear Science and Engineering. 48:319-322 (1972).
3. Evans, R. D. The Atomic Nucleus. New York: McGraw-Hill Book Co., 1955.
4. Grutter, A. and J. C. Shorrocks. "Vapour Pressures of Xenon (77°-180°K) and Krypton (77°-130°K)." Nature 204: 1084-1085 (1964).
5. Horrocks, D. L. and M. H. Studier. "Determination of Radioactive Noble Gases with a Liquid Scintillator." Analytical Chemistry. 36:2077-2079 (1964).
6. Kaplan, I. Nuclear Physics. (Second Edition) Reading, Mass.: Addison-Wesley Publishing Co., Inc., 1962.
7. KeVex-ray Instruction Manual. KeVex Kit, Model 2000. Burlingame, Calif.: KeVex-ray Corp. 1970.
8. KeVex-ray Instruction Manual. X-ray Amplifier, Model 4500. Burlingame, Calif.: KeVex-ray Corp. 1972.
9. Klein, C. A. "Semiconductor Particle Detection: A Reassessment of the Fano Factor Situation." IEEE Transactions on Nuclear Science. NS-18, No. 3.: 214-225 (1968).
10. Langmuir, I. "The Vapor Pressure of Metallic Tungsten." Physics Review. 2:329-342 (1913).
11. Lederer, C. M., et al. Table of Isotopes. (Sixth Edition) New York: John Wiley and Sons, Inc., 1967.
12. Ortec Instruction Manual. Detectors. Oak Ridge, Tenn.: Ortec Inc.
13. Podgurski, H. H. and F. N. Davis. "Thermal Transpiration at Low Pressure. The Vapor Pressure of Xenon Below 90°K." Physical Chemistry. 65:1343-1348 (1961).
14. Price, W. J. Nuclear Radiation Detection. (Second Edition) New York: McGraw-Hill Book Co., 1958.

15. Storm, E. et al. Gamma Ray Absorption Coefficients for Elements 1 to 100. LA-2237.
16. Weast, R. C., editor. Handbook of Chemistry and Physics. (54th Edition) Cleveland, Ohio: CRC Press, 1973.

Appendix A

Pump Rate Determination

To determine the pump rate for a particular situation, it must first be established what type of flow is involved. The Knudsen number can be used to establish the flow characteristics. According to Dushman the limits of the Knudsen number which delineate the ranges of flow type are as follows:

when $L_{a/a} < 0.01$ the flow is viscous

when $L_{a/a} > 1.00$ the flow is molecular

when $0.1 < L_{a/a} < 1.00$ the flow is in the transition range

$$L_a = 8.589 \frac{\eta}{P_{mm}} \left(\frac{T}{M}\right)^{1/2} \text{ cm} \quad (9)$$

where

a = characteristic dimension

η = viscosity in grams/cm-sec

P_{mm} = average pressure in mmHg

T = temperature in °K

M = molecular mass in grams (Ref 1:81)

The gas handling manifold was used in this study to approximate the sample configuration in the original construction of the detection chamber. That is, xenon deposited on an area of 5.1 cm^2 and exposed to a vacuum of 10^{-5} mmHg maintained by Zeolite pellets. The gas-handling manifold configuration is shown in Figure 15. For the situation shown, $L_{a/a}$ is 11.3 which implies molecular flow predominates. Then, for molecular flow in a cylindrical tube whose length is about 100 times the radius:

$$F = 30.48 \frac{a^3}{l} \left(\frac{T}{M}\right)^{1/2} \text{ liters/sec} \quad (\text{Ref 1:88}) \quad (10)$$

In this case, $F = 0.0383$ liters/sec and a liter of xenon at 0.95×10^{-3} mmHg and 295°K contains 6.71×10^{-6} grams. The pump rate is therefore 2.57×10^{-7} gm of Xe/sec.

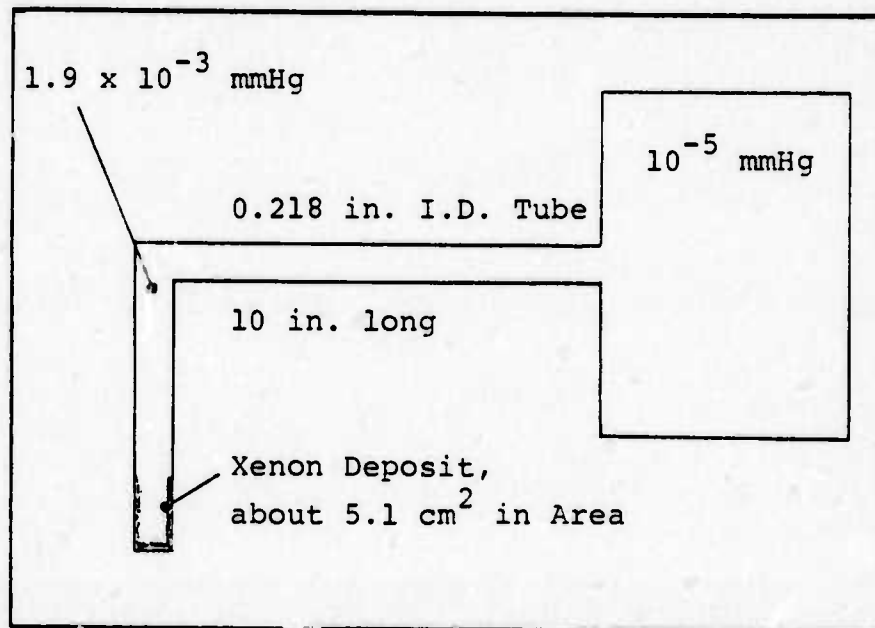


Figure 15. Pump Rate Configuration

Appendix B

Inherent Loss

The procedure for introducing a xenon sample into the detection system and removing it again is as follows.

- 1) The break-seal tube containing the sample is coupled to the system and the upper portion evacuated.
- 2) The seal is broken and the sample transferred into the detection system by cryogenic pumping.
- 3) The used tube is removed and a new break-seal tube is coupled to the system.
- 4) The tube is evacuated and the sample transferred back by cryogenic pumping.
- 5) The tube is flame sealed and removed.

Since cryogenic pumping is used, xenon vapor will permeate the total volume involved. If a portion of the volume is removed, xenon will be lost in proportion to the vapor pressure and the volume lost. In the above procedure, the volume lost includes the volume of a break-seal tube, (3) and the volume of the detection system plus the upper portion of a break-seal tube, (5). The average volume of the break-seal tubes used in this study was about 30 cm^3 . The volume of the valving arrangement and sample chamber is about 8 cm^3 . The vapor pressure of xenon at the cryogenic pumping temperature is $1.9 \times 10^{-3} \text{ mmHg}$. The inherent loss is, therefore, on the order of $6 \times 10^{-7} \text{ gm}$ of Xe, but will vary with the volume of the break-seal tube used.

Appendix C

Effect of Deposition Profile

The data from the experiment to determine the effect of deposition profile is given below.

Table III
Deposition Profile Data

Counts in X-ray Peak		Elapsed Time (min)	Relative Decay- Corrected Counts
1	5431	0	5431
2	5397	14	5401
3	5410	27	5419
4	5398	41	5411
5	5452	55	5470
6	5527	69	5550
7	5553	82	5580
8	5214	96	5243
9	5585	111	5622
10	5494	125	5534
11	5472	140	5517
12	5639	155	5691
13	5548	170	5604
14	5518	185	5578
15	5605	199	5671
16	5554	214	5624
17	5382	229	5455
18	5441	244	5520
19	5355	258	5437
20	5277	272	5362

$$\bar{n} = \frac{\sum_i n_i}{N} = 5506 \quad (11)$$

$$s_n = \left[\frac{\sum_i (n_i - \bar{n})^2}{N - 1} \right]^{1/2} = 113 \quad (12)$$

If the deviation in measurements is due only to the statistical nature of the decay process, one would expect the data to follow a Poisson distribution, ie;

$$s_n \approx \sigma = \sqrt{\bar{n}} \quad \text{and} \quad 0.1 \leq P_\chi(\chi^2, \nu) \leq 0.9$$

For the data set:

$$\sigma = \sqrt{\bar{n}} = 74$$

$$\nu = N - 1 = 19$$

$$\chi_\nu^2 = \left[\frac{\sum_i (n_i - \bar{n})}{\bar{n}} \right] \frac{1}{\nu} = 2.32 \quad (13)$$

$$P_\chi(\chi_\nu^2, \nu) \approx 0.001$$

The extremely low value of P_χ and σ much less than s_n implies the data set does not follow a Poisson distribution. Therefore, statistical fluctuations are probably being introduced by variations in the deposition profile. The repeatability for the number of counts in the K x-ray peaks for the set of data is ± 113 or $\pm 2\%$ for 5506 counts.

Appendix D

Minimum Activity

To determine the counting time required to detect a given sample activity, the criteria of a significance level of 5% for the difference between counts in the peak plus background and background alone is used. The relations used for a significance level in detection of the K_{α_1, α_2} peak are:

$$(N_t - N_b) = 2\sigma(N_t - N_b) \quad (14)$$

$$\sigma(N_t - N_b) = \sqrt{\sigma_{N_t}^2 + \sigma_{N_b}^2} \quad (15)$$

$$\sigma_{N_t} = \sqrt{N_t} \quad (16)$$

$$\sigma_{N_b} = \sqrt{N_b} \quad (17)$$

where

N_t = number of counts in K_{α_1, α_2} peak plus background

N_b = number of counts in background

The following relations also hold:

$$N_t = A\epsilon_x f t + tR_{nbg} + tR_{ebg}$$

$$N_b = tR_{nbg} + tR_{ebg}$$

where

A = activity of sample

ϵ_x = efficiency of system for Xe K X-rays

f = no. of K_{α_1, α_2} per disintegration of Xe^{131m}

t = counting time

R_{nbg} = natural background count rate

R_{ebg} = background count rate due to internal conversion electrons

Combining and transforming the above equations leads to:

$$t = \frac{4(A\epsilon_x f + 2R_{\text{nbg}} + 2R_{\text{ebg}})}{(A\epsilon_x f)^2}$$

A similar equation can be derived for the internal conversion electron peaks, then for a given sample activity the counting time required to establish a significance level of 5% can be calculated. The curves shown in Figure 13 of the System Characteristics section have been calculated from these equations and system/spectrum parameters based on the spectrum of a $\text{Xe}^{131\text{m}}$ sample containing 8.27×10^{-4} gm of xenon at a concentration of 12.8×10^4 DPM/std. cm^3 . The "x-rays" curve is based on detection of the K_{α_1, α_2} x-rays, the "electrons" curve is based on detection of the K internal conversion electrons, and the "x-rays, electrons suppressed" curve is based on the detection of the K_{α_1, α_2} x-rays with the conversion electrons completely eliminated by an absorber.

The pertinent parameters are:

keV/channel	0.224
no. $K_{\alpha_1, \alpha_2}/\text{Xe}^{131\text{m}}$ dis ...	0.592×0.817 (Ref 11:570)
no. $K_{\text{ICe}}/\text{Xe}^{131\text{m}}$ dis	0.681
R_{nbg}	0.07 CPM/keV
ϵ_x	3%
ϵ_{ICe}	14%

Width of K_{α_1, α_2} peak 10 channels

R_{ebg} at K_{α_1, α_2} peak 10 CPM/ch.

Width of K_{ICe} peak 57 channels

R_{ebg} at K_{ICe} peak 7.8 CPM/ch.

Appendix E

Gas Handling Manifold

The gas handling manifold was designed and built to provide the capability of precise mass measurement, dilution, combination, and/or division of gas samples as required for the evaluation of the detection system. A picture of the manifold is presented in Figure 6 and a sketch with the important details labeled is presented in Figure 16. Arabic numerals indicate valves and the lettered items are as follows:

- A Section of manifold whose volume is calibrated
- B Section of manifold whose volume is calibrated
- C Cold finger
- D Cold finger
- E Ion tube
- F Liquid nitrogen trap
- G Diffusion pump
- H Transducer for Pace gauge
- I Hastings gauge
- J Cylinder of non-radioactive xenon
- K Argon line
- L Coupling for break-seal tubes

A brief description of the procedure for introducing a sample into the manifold and determining its mass follows.

- 1) With all valves open except 4, 7, and 8 evacuate the manifold with the diffusion pump and liquid nitrogen trap.

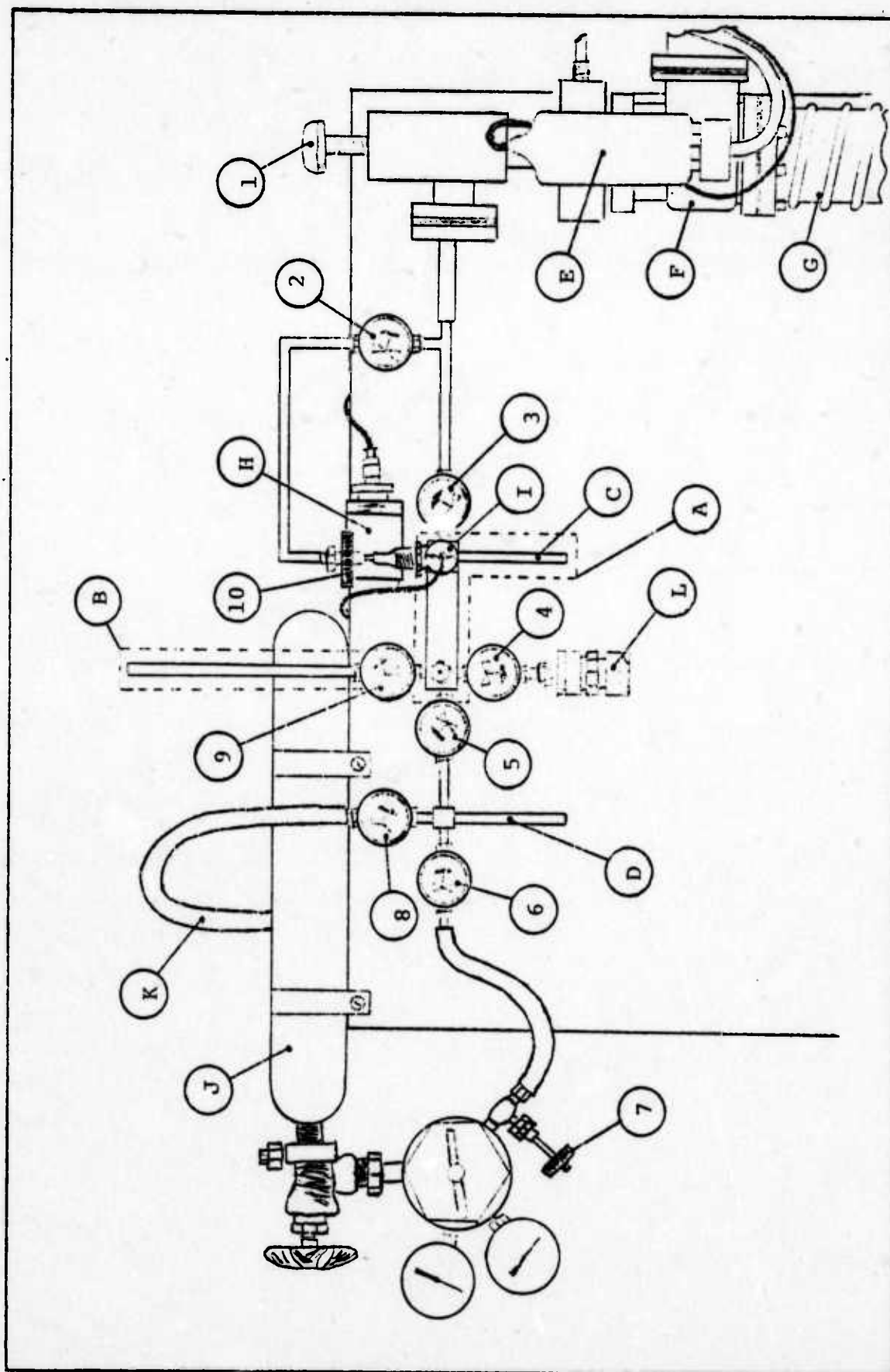


Figure 16. Gas Handling Manifold

- 2) Attach the break-seal tube at coupling L, open valve 4 and evacuate the upper portion of the tube.
- 3) Close all valves except 1, 2 and 4 and cool cold finger C with liquid nitrogen.
- 4) Break the seal in the tube. The xenon will transfer into the manifold and freeze in cold finger C.
- 5) Close valve 4 and allow cold finger C to warm up to room temperature. The pressure of the gas can then be measured with the Pace gauge. Since the temperature, pressure and volume occupied are known, the mass of the sample can be calculated.
- 6) Open valve 5, cool cold finger D and transfer the sample out of section A. After transfer, close valve 5, remove old break-seal tube, attach a new tube, open valves 3 and 4 and evacuate the new tube.
- 7) Close valve 3, cool the new break-seal tube with liquid nitrogen, open valve 5 and allow the sample to transfer into the new tube.
- 8) Keeping the sample frozen in the bottom of the tube, seal the tube off with a torch. Valve 4 can then be closed and the tube disconnected from the system.

Calibrated section B can be used in conjunction with section A to measure large samples or to divide samples. The connection provided to the non-radioactive-xenon cylinder allows dilution of samples if desired and the argon line provides a means of flushing the system. The diffusion pump in conjunction with the liquid nitrogen trap allows evacuation of the manifold to 10^{-7} mmHg as measured with the ion tube and the pressure range of the Pace pressure gauge is ~ 10 to 250 mmHg with one side of the differential transducer referenced to 10^{-7} mmHg through valve 2. In addition, the Hastings gauge allows measurements of pressure in the manifold in the μ Hg range.

Vita

Charles Eugene Rowe was born on 5 July 1946 in Oak Park, Illinois, the son of Melvin C. Rowe and Zelda A. Rowe. After graduating from Fenton High School, Bensenville, Illinois in 1964 he enrolled at DeVry Institute of Technology in Chicago. After graduating from DeVry, he enrolled in the Engineering College of the University of Illinois, Chicago Circle. In 1968, after two years of undergraduate study, he enlisted in the Air Force and subsequently attended Ground Tracking Radar training at Keesler AFB, Mississippi. His next assignment was to the 6596th Instrumentation Sq. at Vandenberg AFB, California. In 1970 he enrolled in the Engineering College of the Arizona State University in Tempe, Arizona and graduated with distinction in 1972. His next assignment was to the Air Force Institute of Technology in 1972.

Permanent address: 402 S. Miner Street
Bensenville, Illinois 60106

This Thesis was typed by Mrs. Laura Reams.

UNCLASSIFIED

SECURITY CLASSIFICATION OF THIS PAGE (When Data Entered)

REPORT DOCUMENTATION PAGE		READ INSTRUCTIONS BEFORE COMPLETING FORM
1. REPORT NUMBER GNE/PH/74-8	2. GOVT ACCESSION NO.	3. RECIPIENT'S CATALOG NUMBER
4. TITLE (and Subtitle) QUANTITATIVE ANALYSIS OF RADIOACTIVE NOBLE GASES WITH A SiLi DETECTOR		5. TYPE OF REPORT & PERIOD COVERED MS Thesis
7. AUTHOR(s) Charles E. Rowe 2nd Lt, USAF		6. PERFORMING ORG. REPORT NUMBER
9. PERFORMING ORGANIZATION NAME AND ADDRESS Air Force Institute of Technology (AFIT-EN) Wright-Patterson AFB, Ohio 45433		8. CONTRACT OR GRANT NUMBER(s) ARPA Order No. 1841
11. CONTROLLING OFFICE NAME AND ADDRESS		10. PROGRAM ELEMENT, PROJECT, TASK AREA & WORK UNIT NUMBERS
14. MONITORING AGENCY NAME & ADDRESS (if different from Controlling Office) Advanced Research Projects Agency of the Department of Defense monitored by HQ USAF (AFTAC/TD-4B)		12. REPORT DATE March, 1974
		13. NUMBER OF PAGES 61
		15. SECURITY CLASS. (of this report) Unclassified
		15a. DECLASSIFICATION/DOWNGRADING SCHEDULE
16. DISTRIBUTION STATEMENT (of this Report) Approved for public release; distribution unlimited		
17. DISTRIBUTION STATEMENT (of the abstract entered in Block 20, if different from Report)		
18. SUPPLEMENTARY NOTES Approved for public release; IAW JERRY C. HIX, Captain, USAF AFR 190-17 Director of Information		
19. KEY WORDS (Continue on reverse side if necessary and identify by block number) Radioactive Noble Gases Xenon SiLi Detector Detection System		
20. ABSTRACT (Continue on reverse side if necessary and identify by block number) A system incorporating a cooled SiLi detector is examined for possible use in the quantitative analysis of radioactive noble gases. In the system, the detector is maintained at liquid nitrogen temperature in a high vacuum environment and cryogenic pumping is used to transfer and isolate gas samples. The gas used in the evaluation of the system is the xenon radionuclide Xe^{131m} . Experimental data and theoretical considerations are used to		

DD FORM 1473

1 JAN 73

EDITION OF 1 NOV 65 IS OBSOLETE

UNCLASSIFIED

SECURITY CLASSIFICATION OF THIS PAGE (When Data Entered)

UNCLASSIFIED

SECURITY CLASSIFICATION OF THIS PAGE(When Data Entered)

✓ establish the relevant characteristics of the system.- Extrapolation of data indicates that in a 10 hour counting time, a significance level of 5% could be established for a Xe^{131m} sample activity of about 25 DPM by internal conversion electron detection or about 90 DPM by x-ray spectroscopy.

SECURITY CLASSIFICATION OF THIS PAGE(When Data Entered)